$\pi \rightarrow \pi^*$ transition intensity and frequency are overestimated by theory: a more detailed CNDO calculation for the ligands themselves including configuration interaction alleviates these problems. The L → M band moves to lower frequency and becomes broader and more intense as n increases.

In general, test results obtained with ab initio ligand molecular orbitals do not differ significantly from results obtained with CNDO. Both methods provide a similar description of the molecular orbital coefficients and of the occupied orbital energies; CNDO calculates the virtual orbital energies at considerably lower energy with smaller spacings, however. Since CNDO is parametrized to provide a good description of the spectroscopy of these molecules, one presumes that its energy levels, when used in conjunction with the simple approximations used herein, are more appropriate than the ab initio levels in this application. Quantitatively, the calculated spectra are quite similar independent of the method used to determine the ligand molecular orbitals. The major difference between the CNDO and ab initio spectra is that the ab initio calculations place much less intensity into the L → M* and M → L* bands and place these bands at higher energy when $n > 0$. Also, it is shown that an appropriate parametrization for the Hückel method can be constructed that leads to quite similar results. From a philosophical perspective, however, it is desirable to use a calculation method that contains no adjustable parameters at all. We are presently looking into ways of adapting programs like CNDO/S-CI[29] and Xα[47] to handle solvent effects and/or second-series transition metals.

The analysis presented for the spectra of the Ru^{III}–Ru^{III} complexes shows unambiguously that a triplet ground state is dominant for these ions at room temperature. Note that symmetry lowering of the singlet state as a result of the torsional motions cannot account for the observed spectra because the ligands, at their most probable configurations, retain enough symmetry to uphold the selection rules displayed in Figure 3.

Because of the uncertainty in the interpretation of the experimental M → M spectrum for $n = 2$, it is not possible to conclude from experiment the nature of the distance dependence of the intramolecular coupling; the experimental results, however, are not inconsistent with the postulate of exponential decay of the coupling with increasing bridge length. Spectra of the highest quality are necessary in order to test out the present theories for long-distance electron-transfer reactions. It is also necessary to take into account effects such as floppy torsional motions, and experimental systems should be designed to control conformation as tightly as is possible.

Theory predicts that the electronic coupling decreases almost exponentially with distance and predicts complexes that will show much slower, less exponential bridge-length dependences. Synthesis of these complexes is of interest because of possible applications to molecular electronic devices,[48] but by nature it will be difficult to deconvolve the intervalence M → M spectra from the overlapping M → L spectra.

The effective coupling seen between the metal orbitals is a function of the nuclear coordinates. This is contrary to the usual notion of electronic spectroscopy that the electronic coupling is largely coordinate independent and arises from the coordinate dependence of the energy gaps of the bridge states that transmit the coupling. Far from resonance between the bridge and the metal states, this effect is not important, but it is very important near resonance regions. It gives rise to different coupling strengths depending upon whether the electron is transferring by thermal or photoinduced mechanisms.

Acknowledgment. We wish to thank Prof. H. Taube (Stanford), Prof. P. Ford (University of Santa Barbara), and Prof. T. J. Meyer (The University of North Carolina) for their helpful discussions and further information on published and unpublished spectral data, Dr. G. B. Bacskay (University of Sydney) for performing the ab initio calculations, and Prof. S. Sternhell, Dr. L. Field, and Dr. P. A. Lay (all of University of Sydney) for stimulating discussions. J.R.R. is indebted to the Australian Research Council for the provision of a Research Fellowship.

(47) Zhang, L. T.; Ko, J.; Ondrechen, M. J. *J. Am. Chem. Soc.* **1987**, *109*, 1666.
(48) Aviram, A. *J. Am. Chem. Soc.* **1988**, *110*, 5687.
(49) Sen, J.; Taube, H. *Acta Chem. Scand.* **1977**, *A33*, 125.
(50) Marchant, J. A.; Matsubara, T.; Ford, P. C. *Inorg. Chem.* **1977**, *16*, 2160.
(51) Matsubara, T.; Ford, P. C. *Inorg. Chem.* **1976**, *15*, 1107.
(52) Richardson, D. E. Unpublished results.
(53) Buckingham, D. A.; Sargeson, A. M. In *Chelating Agents Metal Chelates*; Dwyer, F. P., Mellor, D. P., Eds.; Academic Press: New York, 1964; p 237.

Contribution from the Department of Chemistry and Laboratory for Molecular Structure and Bonding, Texas A&M University, College Station, Texas 77843

New Niobium Complexes of Alkynes. 5. Electronic Structure and Bonding in the Tetranuclear Complex of Niobium $[Nb_4OCl_8\{(PhC)_4\}_2]^{2-}$

F. Albert Cotton* and Xuejun Feng

Received December 20, 1989

Electronic structure and bonding in a newly prepared tetranuclear complex of niobium, $[Nb_4OCl_8\{(PhC)_4\}_2]^{2-}$, are discussed on the basis of molecular orbital calculations by the Fenske–Hall method. The anion consists of a planar, rectangular Nb_4 group with an oxygen atom at the center, and a C-shaped PhC–C(Ph)C(Ph)–CPh chain clasps each short Nb–Nb edge at the middle and lies in a plane perpendicular to the Nb_4O plane. Our study has been mainly focused on the problems related to the unprecedented structural features of the anion, specifically, the Nb–Nb and Nb–O bonding, and the bonding of the C_4Ph_4 unit to the metal atoms. The resulting bonding scheme gives a satisfactory account of the structure and is consistent with the assignment of a formal oxidation state of III to the metal atoms and the existence of strong bonds between the close pairs of metal atoms.

Introduction

Dinuclear complexes of niobium and tantalum with alkynes as bridges have become familiar to us.[1,2] The compounds have discrete RCCR groups strongly bound to the metal atoms and forming bridges across the M–M bonds. The electronic structures of the molecules of this type and, especially, the bonding of alkynes to the metal dimers have been studied in detail and compared with other molecules of similar type but having different metal atoms.[3]

Recent synthetic study in this type of chemistry in this laboratory has been extended to some new niobium compounds that contain a tetranuclear anion, $[Nb_4OCl_8\{(PhC)_4\}_2]^{2-}$.[4] A schematic

(1) Cotton, F. A.; Shang, M. *Inorg. Chem.* **1989**, *29*, 508.
(2) Cotton, F. A.; Hall, W. T. *Inorg. Chem.* **1980**, *19*, 2354.
(3) Cotton, F. A.; Feng, X. Submitted for publication in *Inorg. Chem.*

0020-1669/90/1329-3697$02.50/0 © 1990 American Chemical Society

representation of certain features of this anion is shown as I.

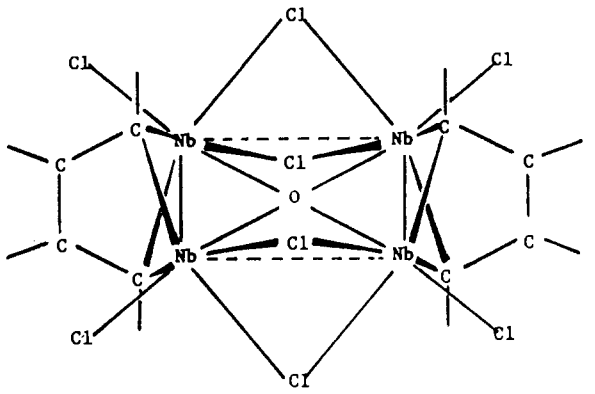

I

There are two major structural features within the anion that have not been encountered previously. The oxygen atom in the anion is centered in a rectangular (not square) plane formed by four metal atoms, and a planar, C-shaped PhC–C(Ph)C(Ph)–CPh chain lies perpendicular to each short Nb–Nb edge with all carbon atoms bonded symmetrically to both metal atoms. This second feature is particularly interesting when compared to the structures of the dinuclear compounds, since the $(CPh)_4$ unit can also be viewed as a bridge across the M–M bond.

The unprecedented structural features just mentioned raise the related questions of how to formulate the bonding of the $(CPh)_4$ units to the metal atoms, how best to assign formal oxidation states to the metal atoms, and what bond orders to assign to the Nb–Nb bonds. We shall answer these questions in the present paper by considering the electronic structure of the $[Nb_4OCl_8(C_4H_4)_2]^{2-}$ ion, which we have obtained from Fenske–Hall molecular orbital calculations.

Computational Procedures

The approximate nonempirical molecular orbital method of Fenske and Hall[5] was employed in the present electronic structure calculations. The calculations were performed for a model system, $[Nb_4OCl_8(C_4H_4)_2]^{2-}$, in which the phenyl groups in $[Nb_4OCl_8\{(PhC)_4\}_2]^{2-}$ were replaced by hydrogen atoms. The model molecule has been assumed to possess ideal D_{2h} symmetry.

The atomic coordinates used in the calculations were obtained from the averaged bond distances and angles for one of the three compounds[4] that contain the $[Nb_4OCl_8\{(PhC)_4\}_2]^{2-}$ ion. The choice was arbitrary since the anion is essentially the same in all three compounds. The bond distances used are as follows: Nb–Nb, 2.6082 Å; Nb–Cl(bridging), 2.601 Å; Nb–Cl(terminal), 2.424 Å; Nb–C(terminal), 2.1325 Å; Nb–O, 2.118 Å; C–H, 1.08 Å. Two nonequivalent C–C distances were used in C_4H_4, namely, 1.464 and 1.453 Å, with C–C–C angles to be 124°.

A right-hand molecular coordinate system was chosen with the oxygen atom at the origin, the metal atoms and terminal Cl atoms in the xy plane, the bridging Cl atoms in the xz plane, and the C_4H_4 units in the yz plane. A right-hand local coordinate system on each metal atom was also chosen as follows. The z axis of the local system points toward the center of the metal plane where the oxygen atom is located, the x axis is in the metal plane, and the y axis is perpendicular to the plane and points to the negative direction of the z axis of the molecular coordinate system. With respect to such coordinate systems, the symmetry classification of the d orbitals of the metal atoms in the molecular D_{2h} point group is given in Table I.

To have a clear description of the bonding of the $(PhC)_4$ units to the metal atoms, the calculations were also carried out for two fragment groups, namely, the Nb_2OCl_8 group and the $(C_4H_4)_2$ group. The fragments retained the same atomic coordinates as they had in the whole system.

Results and Discussion

The upper valence MO levels for $[Nb_4OCl_8(C_4H_4)_2]^{2-}$ are shown in the middle column of Figure 1 with the $13a_g$ orbital as the HOMO. Most of the occupied orbitals that represnt Nb–ligand bonding participate in bonding of the metal atoms to two or more types of ligands, and the following classification of the orbitals highlights their predominant characters. Thus, the occupied orbitals that have been labeled according to the molecular D_{2h} symmetry in this column may be best classified as the Nb–Nb, Nb–C, or Nb–O bonding orbitals and will be discussed in detail. The unlabeled orbitals, on the other hand, represent essentially Nb–Cl bonding or the 3p lone pairs on the Cl atoms. The lower valence MOs that are not shown in the figure are those representing C–C σ and C–H bonding as well as the Cl 3s lone pairs. In addition, the lowest valence MO, the $1a_g$ orbital, provides bonding of the central oxygen atom to the Nb atoms. Listed also in Figure 1 for $[Nb_4OCl_8(C_4H_4)_2]^{2-}$ are the four lowest unoccupied orbitals, which are mainly contributed by the metal d_{yz} orbitals and are antibonding between the metal atoms and the ligands. It is worth mentioning that the electronic structure of the $[Nb_4OCl_8(C_4H_4)_2]^{2-}$ ion has also been calculated by the SCF–Xα–SW method. The results from this calculation are very similar to those obtained by the Fenske–Hall method. The Xα–SW calculation gave an energy gap between the HOMO and the LUMO in the ion of 1.34 eV. The electronic structure and bonding in the ion, however, will be discussed on the basis of the Fenske–Hall molecular orbitals to take advantage of the clear LCAO representation of the MOs.

Table I. Symmetry Classification of Metal d Orbitals

orbital	D_{2h} symmetry			
d_{z^2}	a_g	b_{1g}	b_{2u}	b_{3u}
$d_{x^2-y^2}$	a_g	b_{1g}	b_{2u}	b_{3u}
d_{xy}	b_{2g}	b_{3g}	a_u	b_{1u}
d_{xz}	a_g	b_{1g}	b_{2u}	b_{3u}
d_{yz}	b_{2g}	b_{3g}	a_u	b_{1u}

In Figure 1 we also present the results of the Fenske–Hall MO calculations for the $[Nb_4OCl_8]^{2-}$ and $(C_4H_4)_2$ fragments. The lowest three MOs listed for $[Nb_4OCl_8]^{2-}$ in the first column of the figure have character similar to that of the $6b_{2u}$, $4b_{3u}$, and $5b_{1u}$ orbitals in the second column for $[Nb_4OCl_8(C_4H_4)_2]^{2-}$, namely, bonding between the oxygen atom and the metal atoms. However, the orbitals in the full ion are considerably stabilized relative to the orbitals in the fragment due to the Nb–C bonding character mixed in these orbitals. All other MOs below the $6b_{2u}$ orbital in the first column for $[Nb_4OCl_8]^{2-}$, on the other hand, correlate well with the unlabeled orbitals for $[Nb_4OCl_8(C_4H_4)_2)]^{2-}$.

The calculation on a C_4H_4 group shows that, in addition to the seven orbitals representing the skeletal C–C σ and C–H bonding, the frontier orbitals consist of two π orbitals (π_1 and π_2), two orbitals both having the character of sp^2 hybridization at each end of the carbon chain, and two π^* orbitals. For the two C_4H_4 fragments, jointly, the number of each of the three types of frontier orbitals is simply doubled. These orbitals, labeled according to the molecular D_{2h} symmetry, are shown in the last column of Figure 1 along with schematic drawings for the π and π^* orbitals of a C_4H_4 unit. It may be noted that there is only one set of π^* orbitals listed in the figure. The other set of π^* orbitals is much higher in energy and shows no interaction with the metal atoms.

Bonding of C_4H_4 Units to Nb Atoms. Let us now consider first the bonding of the C_4H_4 units to the metal atoms. It has been pointed out[4] from the structure data of $[Nb_4OCl_8\{(PhC)_4\}_2]^{2-}$ that all C–C distances involving backbone carbon atoms are in the range 1.45–1.52 Å, indicative of single bonds between sp^2-hybridized carbon atoms. If the Ph_4C_4 skeleton is first assembled with such a set of seven C–C σ bonds, the remaining two in-plane sp^2 electrons from the terminal carbon atoms and four π electrons from each carbon in the C_4 chain then have to be assumed to be contributed to Nb–C bonding, in order not to increase the C–C bond order. The present calculations describe clearly how these electrons are diverted into the Nb–C bonding orbitals.

As can be seen in the middle column of Figure 1, the two lowest molecular orbitals listed for $[Nb_4OCl_8(C_4H_4)_2]^{2-}$ are the $3b_{3u}$ and $2b_{1g}$ orbitals. These orbitals have 19% and 12% contributions from the metal atoms, respectively, and remaining contributions are mainly due to the π_1-type orbitals of the C_4H_4 groups. Their

(4) Cotton, F. A.; Shang, M. *J. Am. Chem. Soc.* **1990**, *112*, 1584.
(5) Hall, M. B.; Fenske, R. F. *Inorg. Chem.* **1972**, *11*, 768.

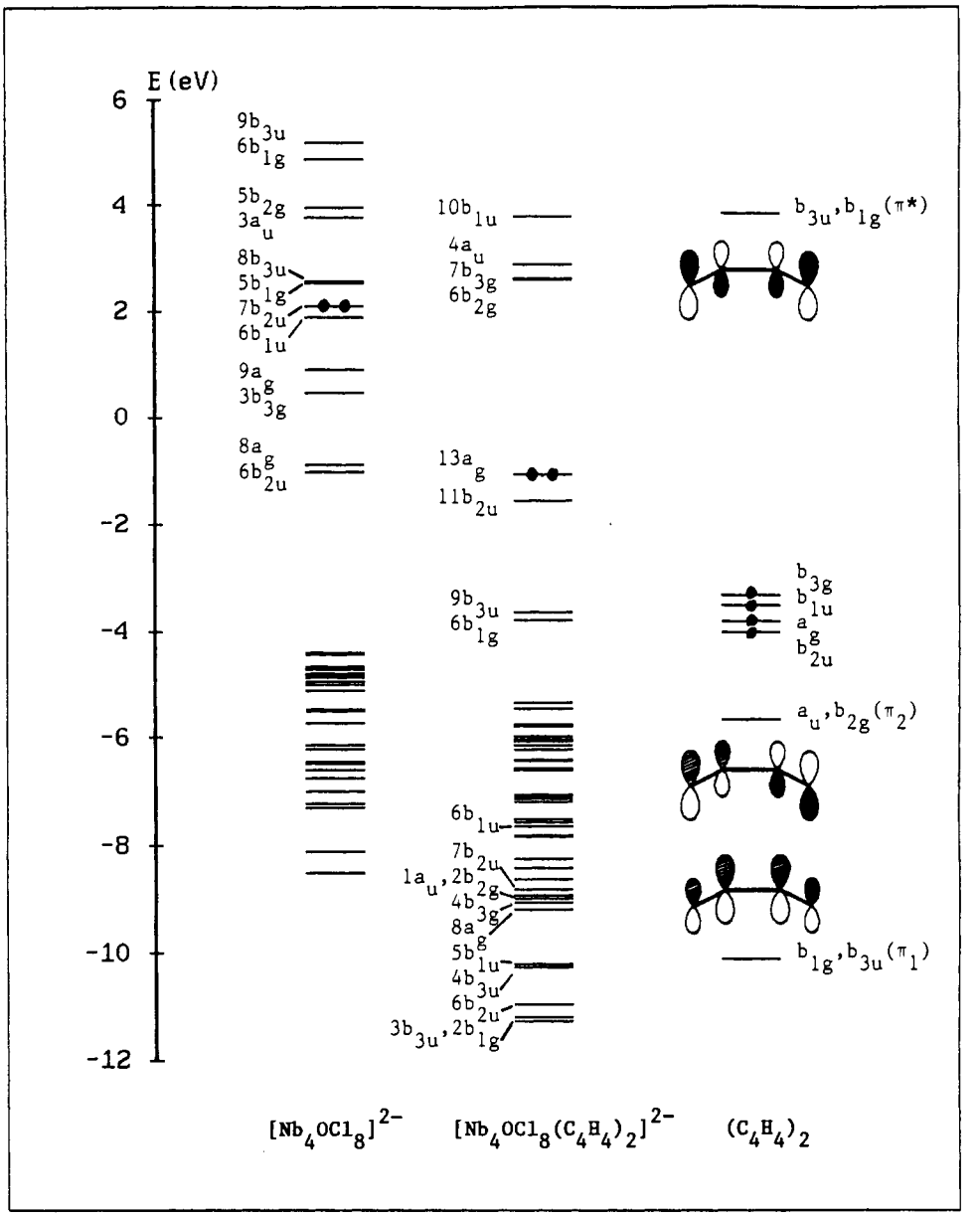

Figure 1. Fenske–Hall molecular orbital diagrams for $[Nb_4OCl_8(C_4H_4)_2]^{2-}$ and the fragments.

essential role is as bonding orbitals between the metal atoms and the C_4H_4 units. These $3b_{3u}$ and $2b_{1g}$ orbitals are directly correlated to the $9b_{3u}$ and $6b_{1g}$ orbitals in the first column of the figure for $[Nb_4OCl_8]^{2-}$. The latter orbitals are predominantly the combinations of the metal d_{xz} orbitals of b_{3u} and b_{1g} symmetries, and both are antibonding between a pair of Nb atoms on the short edge of the Nb_4 rectangular plane and thus are unoccupied. Therefore, the Nb–C bonding carried by the $3b_{3u}$ and $2b_{1g}$ orbitals can be clearly regarded as due to electron donation from the b_{1g} and b_{2u} (π_1) orbitals of the carbon atoms to the metal atoms. A similar situation is found for the $1a_u$ and $2b_{2g}$ orbitals in $[Nb_4OCl_8(C_4H_4)_2]^{2-}$. The contribution to the Nb–C bonding made by these two orbitals is attributable to electron donation from the π_2-type orbitals in the C_4H_4 units to the $3a_u$ and $5b_{2g}$ orbitals in $[Nb_4OCl_8]^{2-}$. The orbitals accepting the π_2 electrons in this case are also empty and of mainly metal character, but they are the antibonding combinations of the d_{xy} and d_{yz} orbitals.

Shown in Figure 2 are the contour plots of the $2b_{1g}$ and $1a_u$ orbitals in $[Nb_4OCl_8(C_4H_4)_2]^{2-}$, which may be taken as illustrative of the Nb–C bonding we just discussed. The contour plot for the $2b_{1g}$ orbital (Figure 2-1) is plotted in the xy plane of the molecular coordinate system that includes the Nb_4 rectangle in it. Since there are no carbon atoms in this plane, there are no symbols to indicate the positions of carbon atoms. However, as can be seen from the figure, the overlap between the d orbitals of the metal

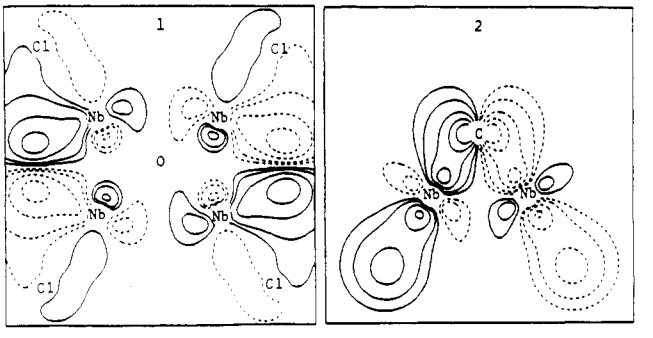

Figure 2. Contour plots with contour values ±0.01, ±0.02, ±0.04, ±0.06, and ±0.08 for (1) the $2b_{1g}$ orbital and (2) the $1a_u$ orbitals in $[Nb_4OCl_8(C_4H_4)_2]^{2-}$. Dashed lines indicate negative contour values.

atoms and the π orbital of $(C_4H_4)_2$ is shown clearly on the left and right sides of the metal rectangle. The contour for the $1a_u$ orbital (Figure 2-2), on the other hand, was plotted in a plane including one terminal carbon atom and a pair of metal atoms on the short edge of the metal rectangle. This plot illustrates very clearly how the carbon atom is bonded to the metal atoms.

It is noted that the $8a_g$ and $6b_{2u}$ orbitals in $[Nb_4OCl_8]^{2-}$ (first column in Figure 1) correlate directly with the $13a_g$ and $11b_{2u}$ orbitals in $[Nb_4OCl_8(C_4H_4)_2]^{2-}$ (middle column). The orbitals

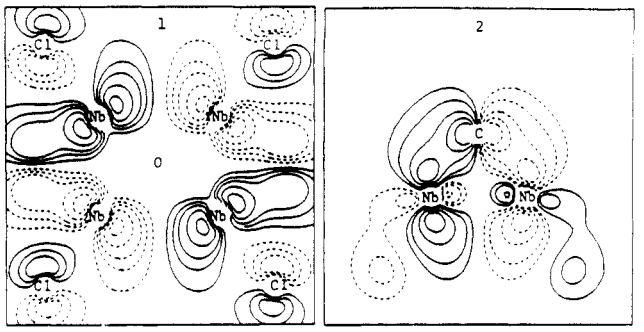

Figure 3. Contour plots for the $6b_{1g}$ orbitals in $[Nb_4OCl_8(C_4H_4)_2]^{2-}$ with the same contour values as in Figure 2.

involving in Nb–Nb bonding will be discussed later. Except for the occupied $8a_g$ and $6b_{2u}$ orbitals, we still have six orbitals that have not been considered yet and eight electrons left in $[Nb_4OCl_8]^{2-}$. These orbitals, namely, the $8b_{3u}$, $5b_{1g}$, $7b_{2u}$, $6b_{1u}$, $9a_g$, and $3b_{3g}$ orbitals, all have predominant contributions due to the metal atoms. On the other hand, the orbitals not considered yet for $(C_4H_4)_2$ are the two empty π^* orbitals (b_{3u} and b_{1g} in symmetry) and the set of four orbitals (b_{3g}, b_{1u}, a_g, and b_{2u} in symmetry) holding four sp^2 electrons in the terminal carbon atoms.

As would be expected, the b_{3u} and b_{1g} π^* orbitals interact strongly with the $8b_{3u}$ and $5b_{1g}$ orbitals of $[Nb_4OCl_8]^{2-}$, leading to a pair of Nb–C bonding orbitals, the $9b_{3u}$ and $6b_{1g}$ orbitals in $[Nb_4OCl_8(C_4H_4)_2]^{2-}$. The $9b_{3u}$ and $6b_{1g}$ orbitals have contributions from the metal atoms (mainly due to the $d_{x^2-y^2}$ orbitals) of 33% and 43%, respectively. It may be noted that the π^* orbitals are originally empty and much higher in energy than other orbitals in $(C_4H_4)_2$. Thus, the electrons filling the $9b_{3u}$ and $6b_{1g}$ orbitals should be regarded as donated by the metal atoms, one electron from each metal atom. It may also be mentioned that both $8b_{3u}$ and $5b_{1g}$ orbitals in $[Nb_4OCl_8]^{2-}$ are antibonding between the pair of Nb atoms on the short edge of the Nb_4 rectangle. However, the Nb–C bonding, due to the overlap between each of them and one of the π^* orbitals, is so strong that the $9b_{3u}$ and $6b_{1g}$ orbitals in $[Nb_4OCl_8(C_4H_4)_2]^{2-}$ lie appreciably below the $13a_g$ and $11b_{2u}$ orbitals, which, as we shall later see, are strongly bonding between the pair of the Nb atoms. The Nb–C bonding characters discussed here are shown graphically by the contour plots for the $6b_{1g}$ orbital in Figure 3. The orbital was plotted in the same two planes as those for the contour plots in Figure 2.

The remaining $7b_{2u}$, $6b_{1u}$, $9a_g$, and $3b_{3g}$ orbitals in $[Nb_4OCl_8]^{2-}$, which all have Nb–Nb bonding character, symmetrically match the set of four orbitals in $(C_4H_4)_2$ with sp^2 character. The fragment orbitals then overlap with each other according their symmetries, resulting in a set of four Nb–C bonding orbitals in $[Nb_4OCl_8\{(PhC)_4\}_2]^{2-}$. These bonding orbitals are shown in the middle column of Figure 1 as the $6b_{1u}$, $7b_{2u}$, $4b_{3g}$, and $8a_g$ orbitals. The metal contributions to the $7b_{2u}$ and $8a_g$ orbitals, mainly from the d_{xz} orbitals, are 28% and 36%, respectively. For the $6b_{1u}$ and $4b_{3g}$ orbitals, the contributions are 16% and 30%, respectively, and are from the d_{xy} and d_{yz} orbitals. If each of these orbitals is regarded formally as representing a bond between one metal atom and one terminal carbon atom, the electrons that fill the orbital then may be regarded as one sp^2 electron from the carbon atom and one from the metal atom. As the examples of this bonding, contour plots for the $8a_g$ and $4b_{3g}$ orbitals are shown in Figure 4-1,2, respectively. They are plotted in the same plane as that in Figure 2-2. The Nb–C bonding is characteristically different from those discussed previously, which can be seen clearly by comparison of Figure 4 with Figure 2-2 and Figure 3-2.

Bonding in the Nb_4O Rectangle. The central oxygen atom in the $[Nb_4OCl_8\{(PhC)_4\}_2]^{2-}$ ion has an environment that is without precedent, so far as we know. It is bonded to four metal atoms in a rectangular (not square) plane. Our calculation for $[Nb_4OCl_8(C_4H_4)_2]^{2-}$ shows that the orbitals responsible for the bonding of the oxygen atom to the four metal atoms are the $5b_{1u}$, $4b_{3u}$, and $6b_{2u}$ orbitals as listed in Figure 1, plus the $1a_g$ orbital, which is the lowest valence orbital and not listed. As will be seen

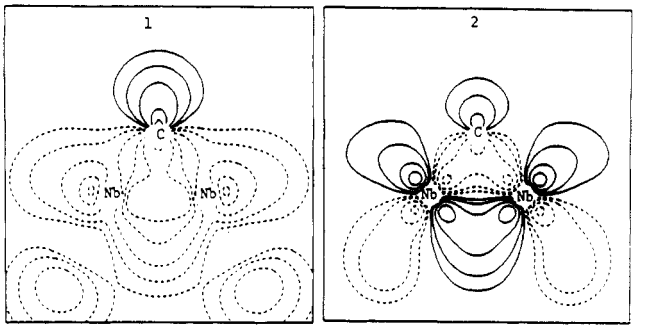

Figure 4. Contour plots for (1) the $8a_g$ orbital (contour values ±0.005, ±0.01, ±0.02, ±0.04, ±0.06) and (2) the $4b_{3g}$ orbitals (same contour values as in Figure 2) in $[Nb_4OCl_8(C_4H_4)_2]^{2-}$.

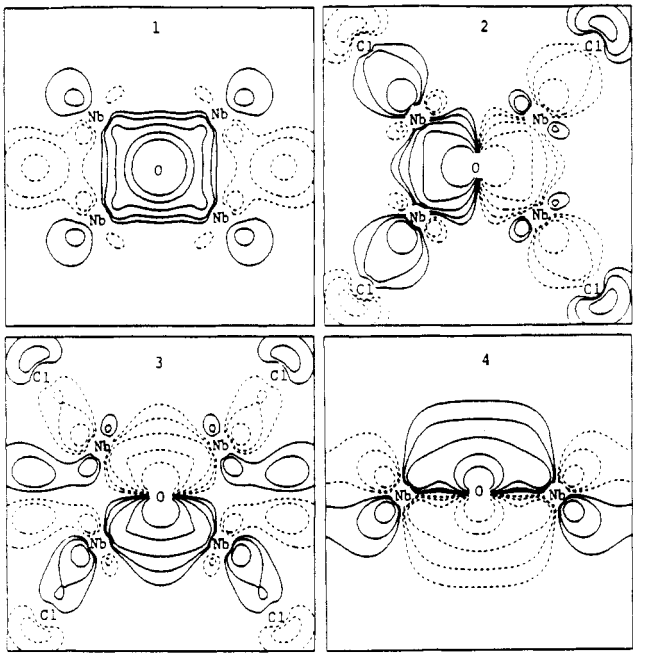

Figure 5. Contour plots for (1) the $1a_g$ orbital, (2) the $6b_{2u}$ orbitals, (3) the $4b_{3u}$ orbital, and (4) the $5b_{1u}$ orbital in $[Nb_4OCl_8(C_4H_4)_2]^{2-}$, with contour values for all four being ±0.01, ±0.02, ±0.04, ±0.08, and ±0.16.

below, the Nb–O bonding scheme is relatively straightforward compared to the Nb–C bonding.

For the oxygen atom at the origin of the chosen molecular coordinate system, the 2s, $2p_x$, $2p_y$, and $2p_z$ orbitals belong to the a_g, b_{3u}, b_{2u}, and b_{1u} representations of the D_{2h} molecular point group, respectively. Thus, the oxygen 2s orbital can interact strongly with the set of four d_{z^2} orbitals of the metal atoms, which are combined with a_g symmetry and point to the center of the metal plane. This results in the lowest bonding orbital in $[Nb_4OCl_8(C_4H_4)_2]^{2-}$, as shown in Figure 5-1. The $2p_y$ orbital of the oxygen atom is oriented toward the centers of each short Nb–Nb edge and overlaps well with the combination of metal d_{z^2} orbitals of b_{2u} symmetry, as shown by the contour plot for the $6b_{2u}$ orbital in Figure 5-2. The shape of the $4b_{3u}$ orbital is similar to that of the $6b_{2u}$ orbital, but turned 90°, as can be seen from Figure 5-3. It results from the interaction of the oxygen $2p_x$ orbital with the d_{z^2} combination of b_{3u} symmetry. The oxygen $2p_z$ orbital, on the other hand, is perpendicular to the metal plane and overlaps with a set of four d_{yz} orbitals of the metal atoms combined in accord with b_{1u} symmetry. This gives the $5b_{1u}$ orbital, which is plotted in Figure 5-4 in a plane perpendicular to the metal plane and passing through the oxygen atom and two metal atoms on a diagonal of the metal rectangle.

If the central oxygen is formally considered as an O^{2-} ion, then all of its eight valence electrons are used in forming the Nb–O bonds. It should be also pointed out that the bonding scheme just described would also apply to a square Nb_4O group. The rectangular Nb_4O structure in $[Nb_4OCl_8\{(PhC)_4\}_2]^{2-}$ has to be

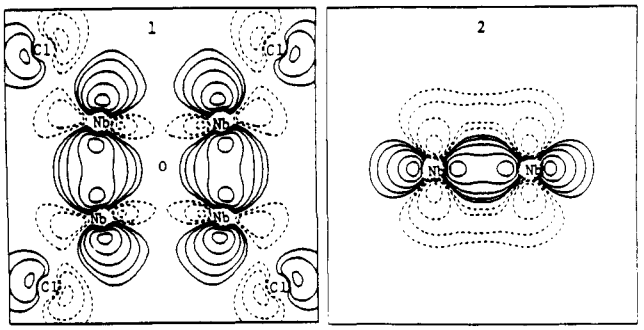

Figure 6. Contour plots for the $13a_g$ orbital in $[Nb_4OCl_8(C_4H_4)_2]^{2-}$ with the same contour values as in Figure 5.

considered as a consequence of the alternating Nb–Nb-bonded and $Nb(\mu\text{-}Cl)_2Nb$ edges.

Nb–Nb Bonding. It was previously[4] suggested, in purely qualitative terms, that by regarding the $(CPh)_4$ ligand as formally dinegative and consisting of two halves each of which serves as a 3-electron bridging ligand (like Cl^-), the two halves of the $[Nb_4OCl_8\{(PhC)_4\}_2]^{2-}$ ion could be regarded as face-sharing bioctahedra that share the bridging Cl atoms and the central oxygen atom. On this basis, the niobium atoms have a formal oxidation number of III and the Nb–Nb bonds are double bonds. Let us now see whether the calculations provide any support for this suggestion.

We begin by looking for orbitals that are mainly metal atom based and localized between or across the pairs of metal atoms that form the short edges of the Nb_4 rectangle. We find two such orbitals, $11b_{2u}$ and $13a_g$, which have 83% and 73% metal contributions, respectively. Contour diagrams of the $13a_g$ orbital are shown in Figure 6 and the $11b_{2u}$ orbital has a very similar appearance except that the major lobes are negative on one side and positive on the other, instead of positive on both as in Figure 6. In each MO the major contributions are from overlaps between $d_{x^2-y^2}$ orbitals supplemented by a little d_{xz} character. Clearly, these two orbitals, each containing two electrons, constitute the MO equivalent of two strong Nb–Nb σ bonds.

However, there are no other orbitals that are also of clear and simple Nb–Nb bonding character. Additional Nb–Nb π bonding could be assumed to occur because of the shortness of the distance, 2.61 Å, but it must be distributed over several MOs and mixed with the bonding between the Nb atoms and the $(PhC)_4$ bridging units. The situation may be compared with a similar case in the diniobium complex $Nb_2Cl_4O(PhCCPh)(THF)_4$.[1,3] Our calculation[3] indicated that a full strength Nb–Nb π bond in this molecule can hardly be expected, and the relatively short Nb–Nb distance, 2.74 Å, can be considered to be the result of the strong binding of the $(PhC)_2$ unit to the Nb dimer. It is clear that the bonding interaction of the $(PhC)_4$ unit with the pair of Nb atoms in the tetramer is much stronger than the Nb–C bonding in the dimer. Therefore, the short Nb–Nb distance in the tetramer may be mainly attributed to the $(PhC)_4$ bridge strongly binded to the close pair of Nb atoms, in addition to the strong σ bond. On the other hand, it still seems reasonable, from the Nb–C bonding scheme discussed earlier, to regard the metal atoms as being effectively in formal oxidation states of III.

Acknowledgment. We thank The Robert A. Welch Foundation for support under Grant No. A-494.

Contribution from the Departments of Chemistry, North Carolina State University, Raleigh, North Carolina 27695-8204, and Clemson University, Clemson, South Carolina 29634-1905

Role of the LUMO in Determining Redox Stability for 2,3-Dipyridylpyrazine- and 2,3-Dipyridylquinoxaline-Bridged Ruthenium(II) Bimetallic Complexes

J. B. Cooper,† D. B. MacQueen,‡ J. D. Petersen,‡ and D. W. Wertz*,†

Received November 21, 1989

The cyclic voltammograms (CV) of $[Ru(bpy)_2]_2dpq^{4+}$ and $[Ru(bpy)_2]_2dpp^{4+}$ (dpp = 2,3-dipyridylpyrazine, dpq = 2,3-dipyridylquinoxaline, bpy = 2,2′-bipyridine) indicate six reversible reductions for each species in *N,N*-dimethylformamide (DMF). The resonance Raman (RR), electronic, and ESR spectra indicate that the first two electrons enter a redox orbital (LUMO) that is bridging ligand localized, while the next four electrons enter bpy-localized orbitals. The RR and ESR data and the separation between the two bridging ligand reduction potentials are all consistent with a redox orbital that is predominantly localized on the quinoxaline portion of the ligand for $[Ru(bpy)_2]_2dpq^{4+}$ but involves both the pyridyl and pyrazine portions of the bridge in $[Ru(bpy)_2]_2dpp^{4+}$. The irreversibility of the CV for the doubly reduced dpp complex in CH_3CN is interpreted in terms of a bridging ligand rearrangement involving the pyridyl rings and a breaking of a Ru–N bond upon the addition of the second electron. The redox stability of the dpq complex is attributed to a polarization of the LUMO away from the pyridyl rings toward the fused benzo ring.

Introduction

Complexes of the type $[Ru(bpy)_2]_2BL^{4+}$ (where BL is a π-delocalized tetraimine bridging ligand and bpy is 2,2′-bipyridine) have recieved a great deal of attention recently.[1-20] Although bimetallic species offer the possibility of 2-photon excitation, double chelation of the $Ru(bpy)_2^{2+}$ moieties to the bridging ligand results in a strong perturbation on the bridging ligand π system, usually resulting in a decrease or loss of luminescence with respect to the monometallic species.[2,5,6,14-16] Special emphasis has been placed to relating this loss to the degree of metal–metal communication mediated by the bridging ligand, and interpretation of spectroscopic and electrochemical data has led to several theories regarding the degree of communication between metal centers in such complexes.[6,13-15]

†North Carolina State University.
‡Clemson University.

(1) Braunstein, C. H.; Baker, A. D.; Strekas, T. C.; Gafney, H. D. *Inorg. Chem.* **1984**, *23*, 857.
(2) Dose, E. V.; Wilson, L. J. *Inorg. Chem.* **1978**, *17*, 2660.
(3) Humziker, B.; Ludi, A. *J. Am. Chem. Soc.* **1977**, *99*, 7370.
(4) Ruminski, R. R.; Petersen, J. D. *Inorg. Chem.* **1982**, *21*, 3706.
(5) Rillema, D. P.; Mack, K. B. *Inorg. Chem.* **1982**, *21*, 3849.
(6) Petersen, J. D. In *Supramolecular Photochemistry*; Balzani, V., Ed.; Reidel: Norwell, MA, 1987; p 135.
(7) Ernst, S.; Kaim, W. *Angew. Chem., Int. Ed. Engl.* **1985**, *24*, 430.
(8) Ernst, S.; Kaim, W. *J. Am. Chem. Soc.* **1986**, *108*, 3578.
(9) Kaim, W.; Kohlman, S. *Inorg. Chem.* **1987**, *26*, 68.
(10) Ernst, S.; Kaim, W. *Inorg. Chem.* **1989**, *28*, 1520.
(11) De Cola, L.; Barigelletti, F. *Gazz. Chim. Acta* **1988**, *118*, 417.
(12) Campagna, S.; Denti, G.; DeRosa, G.; Sabatino, L.; Ciano, M.; Balzani, V. *Inorg. Chem.* **1989**, *28*, 2565.
(13) Sahai, R.; Morgan, L.; Rillema, P. *Inorg. Chem.* **1988**, *27*, 3495.

0020-1669/90/1329-3701$02.50/0 © 1990 American Chemical Society